YANG, J., WANG, S., CHEN, L., QIAO, J., FERNANDEZ, C. and GUERRERO, J.M. 2023. High-precision state of charge estimation of lithium-ion batteries based on joint compression factor particle swarm optimization-forgetting factor recursive least square-adaptive extended Kalman filtering. *Journal of The Electrochemical Society* [online], 170(6), article 060527. Available from: https://doi.org/10.1149/1945-7111/acd815

High-precision state of charge estimation of lithium-ion batteries based on joint compression factor particle swarm optimization-forgetting factor recursive least square-adaptive extended Kalman filtering.

YANG, J., WANG, S., CHEN, L., QIAO, J., FERNANDEZ, C. and GUERRERO, J.M.

2023

High-precision State of Charge Estimation of Lithium-ion Batteries Based on Joint Compression Factor Particle Swarm Optimization-Forgetting Factor Recursive Least Square-Adaptive Extended Kalman Filtering

Journal:	*Journal of The Electrochemical Society*
Manuscript ID	JES-110081.R1
Manuscript Type:	Research Paper
Date Submitted by the Author:	09-May-2023

Complete List of Authors:	Yang, Junjie; Southwest University of Science and Technology, Wang, Shunli; Southwest University of Science and Technology, Chen, Lei; Southwest University of Science and Technology Qiao, Jialu; Southwest University of Science and Technology Fernandez, Carlos; Robert Gordon University Guerrero, Josep M.; Aalborg University Department of Energy Technology

Keywords:	lithium-ion battery, state of charge, Energy Storage

High-precision State of Charge Estimation of Lithium-ion Batteries Based on Joint Compression Factor Particle Swarm Optimization-Forgetting Factor Recursive Least Square-Adaptive Extended Kalman Filtering

Junjie Yang,[1] Shunli Wang,[1,z] Lei Chen,[1] Jialu Qiao,[1] Carlos Fernandez,[2] and Josep M. Guerrero[3]

[1]School of Information Engineering, Southwest University of Science and Technology, Mianyang 621010, China
[2]School of Pharmacy and Life Sciences, Robert Gordon University, Aberdeen AB10-7GJ, United Kingdom
[3]Department of Energy Technology, Aalborg University, Pontoppidanstraede 111 9220 Aalborg East, Denmark

[z]E-mail: wangshunli@swust.edu.cn

Abstract: Accurate state of charge (SOC) estimation is an important basis for battery energy management and the applications of lithium-ion batteries. In this paper, an improved compression factor particle swarm optimization-forgetting factor recursive least square (CFPSO -FFRLS) algorithm is proposed, in which the forgetting factor is optimized to identify more accurate parameters for high-precision SOC estimation of lithium-ion battery. In order to improve the SOC estimation accuracy, a dual noise update link is introduced to the traditional extended Kalman filter (EKF), which enhances the algorithm's ability to adapt to noise by updating the process and measurement noises in real time. The experimental results of parameter identification and SOC estimation show that the CFPSO-FFRLS algorithm proposed significantly improves the accuracy of parameter identification, and the joint CFPSO-FFRLS-AEKF algorithm can accurately estimate the SOC of lithium-ium battery under different working conditions. Under HPPC, BBDST and DST working conditions, the mean absolute errors of SOC estimation are 1.14%, 0.78% and 1.1%, which are improved by 42.71%, 65.79% and 39.56% compared with FFRLS-EKF algorithm, and the root mean square errors are 1.18%, 0.99% and 1.11%, improved by 44.86%, 65.98% and 51.74%, respectively.

1. Introduction

Energy security and environmental protection are problems facing the world at present. The emergence of new energy vehicles has realized the problem of combining environmental protection with energy to reduce environmental pollution[1; 2]. Because of the advantages of high energy density, no environmental pollution, long service life and high performance, lithium-ion batteries have played an important role in new energy and other fields and attracted extensive attention[3-5]. As lithium-ion batteries become more and more important in the field of new energy, more and more attention is paid to the real-time monitoring[6]. The accurate state of charge (SOC) estimation of lithium-ion batteries is of great significance in the theoretical research and practical application of lithium-ion batteries.

The establishment of an equivalent model that can accurately characterize the working characteristics of lithium-ion batteries plays an important role in the SOC estimation of lithium-ion batteries[7]. After building a suitable circuit model, the model needs to be identified with parameters[8; 9]. Due to the complex internal structure of lithium-ion batteries, lithium-ion batteries often exhibit strong nonlinear characteristics under complex working conditions, which makes it difficult for traditional equivalent models to accurately characterize the working characteristics of lithium-ion batteries[10]. Therefore, for the SOC estimation of lithium-ion battery, it is necessary to establish an equivalent circuit model that can accurately characterize its working characteristics according to the lithium-ion battery, and then select appropriate algorithms for parameter identification and SOC estimation of lithium-ion battery on this basis[11; 12]. In practice, to accurately estimate the SOC of lithium-ion battery, it is necessary to consider all possible problems and choose appropriate methods based on unpredictable factors.

The accurate parameter identification of the battery model plays a key role in the SOC estimation of the battery. The recursive least square (RLS) algorithm is widely used for parameter identification because of its fast convergence speed and small computational complexity, but it has the problem of data saturation[13-15].

Forgetting factor recursive least square (FFRLS) algorithm introduces a forgetting factor based on traditional RLS algorithm to solve the problem that the recursive results can not reflect the new data because of the accumulation of old data[16]. However, the fixed forgetting factor does not have a good estimation effect in the complex working conditions. One of the improved FFRLS algorithms is the gradient descent optimized FFRLS, which is robust against outliers of model parameters, but the algorithm needs many iterations to achieve sufficient accuracy in some cases[17].

The accuracy of SOC estimation directly affects the output characteristics, service life and safety performance of lithium-ion batteries. There are a variety of SOC estimation methods for lithium-ion batteries according to different situations[18-20]. At present, the common SOC estimation methods for lithium-ion batteries include ampere hour integration method, open circuit voltage method, Kalman filtering algorithm and neural network method and so on[21-23]. The ampere hour integration method is widely used in engineering, but as an open-loop estimation method, with the accumulation of estimation time, the error of its estimated SOC will gradually accumulate, resulting in the inability to meet the requirements of estimation accuracy, and the estimated SOC of this method is greatly affected by the initial value of SOC[24; 25]. The open circuit voltage method is not suitable for online real-time measurement because the battery needs to be kept for a long time to reach a stable state before measurement[26]. The accuracy of the battery model is not required for the neural network method to estimate the SOC of lithium-ion battery, such as BP neural network and LSTM, which are applied in Battery SOC estimation[27; 28]. However, the neural network methods need a large number of sample data as support, and the accuracy of the neural network trained by this method can not be guaranteed[29; 30]. The Kalman filtering algorithm is based on the state-space model of the battery, and it estimates the SOC of the battery by recursion and iteration[31-33]. The Kalman filtering algorithm has a strong correction effect on the initial value error of the system state, and it can also suppress the system noise well[34].

The Kalman filtering algorithm has both strengths and weaknesses when compared with other algorithms.

The conventional Kalman filtering algorithm is only applicable to the state variable estimation of linear systems, and the nonlinear characteristics of lithium-ion batteries lead to the inability of the general Kalman filtering algorithm to estimate their SOC[35; 36]. The cubature Kalman filter for SOC estimation of lithium-ion batteries has good accuracy and fast convergence speed, but it can be sensitive to noise and yield inaccurate results[37; 38]. The extended Kalman filtering (EKF) algorithm, which is introduced based on the Kalman filtering algorithm, can estimate the state of charge of a lithium-ion battery due to its Taylor series expansion of the nonlinear system around the target estimation, omitting the above-quadratic term[39-41]. However, the standard EKF algorithm also has certain problems[42]. Because its noise value is usually fixed, which is inconsistent with the statistical characteristics of the noise of the actual lithium-ion battery under various operating conditions[43-45]. The effect of noise then causes the standard EKF algorithm, like the traditional Kalman filtering algorithm, to fail to resolve the problem of different estimation results due to the effect of noise.

In this paper, the second-order RC equivalent circuit model of ternary lithium-ion battery is established to characterize the operating characteristics of the battery, and an improved compression factor particle swarm optimization-forgetting factor recursive least square (CFPSO-FFRLS) algorithm is proposed to accurately identify the parameters of lithium-ion battery by optimizing the forgetting factor in the FFRLS algorithm. For the SOC estimation, an improved dual noise update link is added to the traditional EKF algorithm to update the process noise and measurement noise, so that the improved adaptive extended Kalman filtering (AEKF) algorithm with dual noise update can adapt to the noise in the estimation process to obtain better estimation results. The parameter identification results of FFRLS, PSO-FFRLS and CFPSO-FFRLS algorithms are obtained and analyzed under hybrid pulse power characteristic (HPPC), Beijing bus dynamic stress test (BBDST) and dynamic stress test (DST) working conditions. The SOC estimation based on FFRLS-EKF, PSO-FFRLS-AEKF and CFPSO-FFRLS-AEKF algorithms are constructed under different working conditions. Finally, the SOC estimation results of the three algorithms are compared and analyzed.

2. Mathematical analysis

2.1. The second-order RC equivalent circuit modeling

The establishment of lithium-ion battery model plays an important role in estimating the SOC of lithium-ion battery. The selection of the battery model needs to comprehensively consider and analyze the accuracy, complexity and the degree of characterization of the battery characteristics of the model. Nowadays, the commonly used battery model is the equivalent circuit model.

Compared with other equivalent circuit models, the second-order RC equivalent circuit model can better characterize the dynamic characteristics of the battery, and the amount of calculation is small, so it has a wide range of applications. In this paper, considering the accuracy and calculation amount of each model, the second-order RC equivalent circuit model is constructed, and the second-order RC equivalent circuit model is shown in Figure 1.

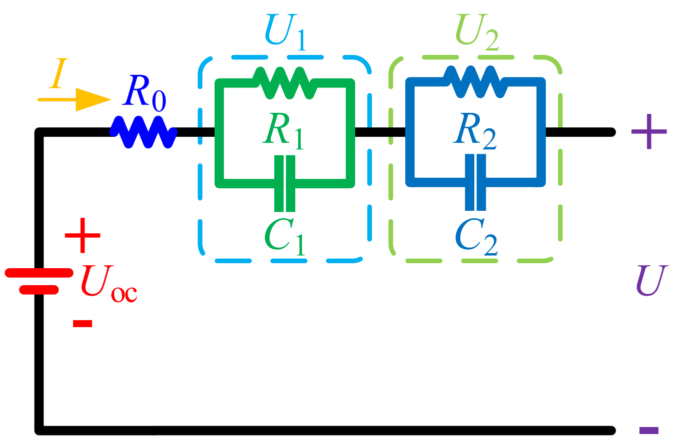

Figure 1. Second-order RC equivalent circuit model

In Figure 1, U_{oc} represents the open circuit voltage of the battery, U represents the terminal voltage, R_0 is the ohmic internal resistance of the battery, R_1 and R_2 represent the internal polarization resistance of the battery, C_1 and C_2 represent the internal polarization capacitance of the battery. This model uses two RC parallel circuits to describe the electrochemical polarization and concentration polarization of the battery, and the terminal voltage of two RC circuits are represented as U_1 and U_2. According to Kirchhoff's circuit law, the second-order equivalent circuit model is analyzed, and the voltage and current expressions of second-order RC equivalent circuit model are obtained, as shown in Equation (1).

$$\begin{cases} U = U_{oc} - IR_0 - U_1 - U_2 \\ \dfrac{dU_1}{dt} = -\dfrac{U_1}{C_1 R_1} + \dfrac{I}{C_1} \\ \dfrac{dU_2}{dt} = -\dfrac{U_2}{C_2 R_2} + \dfrac{I}{C_2} \end{cases} \tag{1}$$

In the equivalent circuit model, the state variable SOC can be used to characterize the open circuit voltage U_{oc} of the lithium-ion battery. Combined with the SOC definition expression shown in Equation (2) of the lithium-ion battery, the SOC of the battery and the voltage of the two RC circuits are taken as the state variables, and the circuit voltage equation of the battery model is taken as the observation equation. The second-order RC equivalent circuit model is discretized, and the discrete state equation is established, as shown in Equation (3) and (4).

$$SOC = SOC_0 - \frac{1}{Q_N}\int \eta I dt \tag{2}$$

$$\begin{bmatrix} SOC_{k+1} \\ U_{1,k+1} \\ U_{2,k+1} \end{bmatrix} = \begin{bmatrix} 1 & 0 & 0 \\ 0 & e^{-\frac{\Delta t}{R_1 C_1}} & 0 \\ 0 & 0 & e^{-\frac{\Delta t}{R_2 C_2}} \end{bmatrix} \begin{bmatrix} SOC_k \\ U_{1,k} \\ U_{2,k} \end{bmatrix} + \begin{bmatrix} -\dfrac{\eta \Delta t}{Q_N} \\ R_1(1-e^{-\frac{\Delta t}{R_1 C_1}}) \\ R_2(1-e^{-\frac{\Delta t}{R_2 C_2}}) \end{bmatrix} I_k + \begin{bmatrix} w_{1,k} \\ w_{2,k} \\ w_{3,k} \end{bmatrix} \tag{3}$$

$$U_k = U_{oc,k} - R_0 I_k + \begin{bmatrix} 0 \\ -1 \\ -1 \end{bmatrix}^T \begin{bmatrix} SOC_k \\ U_{1,k} \\ U_{2,k} \end{bmatrix} + v_k \tag{4}$$

Wherein, η is the Coulomb efficiency of the battery (usually 1), Q_N is the rated capacity constant of the battery, I is the operating current in the circuit, Δt is the sampling interval, w is the state error, and v is the measurement error, respectively.

2.2. Improved CFPSO-FFRLS algorithm for parameter identification

With the increase of recursion times, the old data in RLS algorithm will gradually accumulate, which will submerge the new data information, and finally lead to data saturation in the algorithm, which makes parameter estimation difficult. Therefore, in order to reduce the impact of old data on the current time estimation, the forgetting factor is introduced to the RLS algorithm, and the original outdated data is weighted to reduce its impact on parameter estimation and enhance the influence of new data. The recursive steps of FFRLS algorithm are shown as follows.

(1) Parameters initialization:

$$\begin{cases} \hat{\theta}(0) = \dfrac{1}{\delta}[1,1,1]^T \\ P(0) = \delta I \end{cases} \tag{5}$$

(2) Calculating the estimation error:

$$e(k) = y(k) - \varphi^T(k)\hat{\theta}(k-1) \tag{6}$$

(3) Calculating the gain matrix:

$$K(k) = \frac{P(k-1)\varphi(k)}{\lambda + \varphi^T(k)P(k-1)\varphi(k)} \tag{7}$$

(4) Parameter estimation:

$$\hat{\theta}(k) = \hat{\theta}(k-1) + e(k)K(k) \tag{8}$$

(5) Updating the covariance matrix:

$$P(k) = \frac{1}{\lambda}\left[I - K(k)\varphi^T(k)\right]P(k-1) \tag{9}$$

In the above Equations: $\hat{\theta}$ is the identified parameter vector, δ is the larger positive number set, e is the estimated error, K is the system gain matrix, P is the covariance matrix, λ is the forgetting factor, and I is the unit matrix.

Compared with RLS algorithm, FFRLS algorithm has better estimation ability. However, the FFRLS algorithm usually takes a fixed forgetting factor for parameter identification of the battery, which does not guarantee that the optimal forgetting factor is taken at every moment. To solve this problem, the particle swarm optimization (PSO) algorithm is introduced to optimize the forgetting factor in real time and dynamically evaluate the fitmess value of the forgetting factor at each moment. The update equations for velocity and position of the particles in PSO algorithm are shown in Equation (10).

$$\begin{cases} v_{ij}(t+1) = v_{ij}(t) + c_1 r_1(t)\left[p_{ij}(t) - x_{ij}(t)\right] + c_2 r_2(t)\left[p_{gj}(t) - x_{ij}(t)\right] \\ x_{ij}(t+1) = x_{ij}(t) + v_{ij}(t+1) \end{cases} \tag{10}$$

In Equation (10), c_1 and c_2 are acceleration constants, v_{ij} is the velocity of the particle, x_{ij} is the position of the particle, p_{ij} is the individual optimal position, and p_{gj} is the global optimal position. In this research, the minimum terminal voltage error is taken as the optimization objective, as shown in Equation (11).

$$J = \left| U(k) - \varphi^T(k)\hat{\theta}(k-1) \right| \tag{11}$$

The introduction of weighting factor in the basic PSO algorithm can regulate the global and local search ability of the algorithm. However, the value of inertia weight is often difficult to determine in the practical application of the algorithm, which means the local convergence and global convergence are difficult to balance in the basic PSO algorithm. Therefore, a compression factor is introduced to optimize the final convergence. The velocity update equation of the improved compression factor particle swarm optimization algorithm and the expression for the compression factor are shown in Equation (12) and Equation (13).

$$v_{id}(t) = \lambda v_{id}(t) + c_1 r_1(t)\left[p_{id}(t) - x_{id}(t)\right] + c_2 r_2(t)\left[p_{gd}(t) - x_{id}(t)\right] \tag{12}$$

$$\lambda = \frac{2}{\left| 2 - s - \sqrt{\left(s^2 - 4s\right)} \right|} \tag{13}$$

Wherein, λ is the compression factor introduced in this paper, which is improved from the inertia weight, s is the sum of c_1 and c_2. The inertia weight of the CFPSO algorithm determines the global and local optimization capability of the algorithm, and optimizing it into a compression factor can better balance the development and exploration capabilities of the algorithm. The optimized CFPSO algorithm is capable of efficiently exploring diverse regions to obtain high-quality solutions.

By optimizing the forgetting factor of FFRLS with the CFPSO algorithm, the optimal value of forgetting factor can be found more accurately. The CFPSO-FFRLS algorithm greatly improves the estimation precision of parameter identification. The parameter identification flow chart based on CFPSO-FFRLS algorithm is shown in Figure 2.

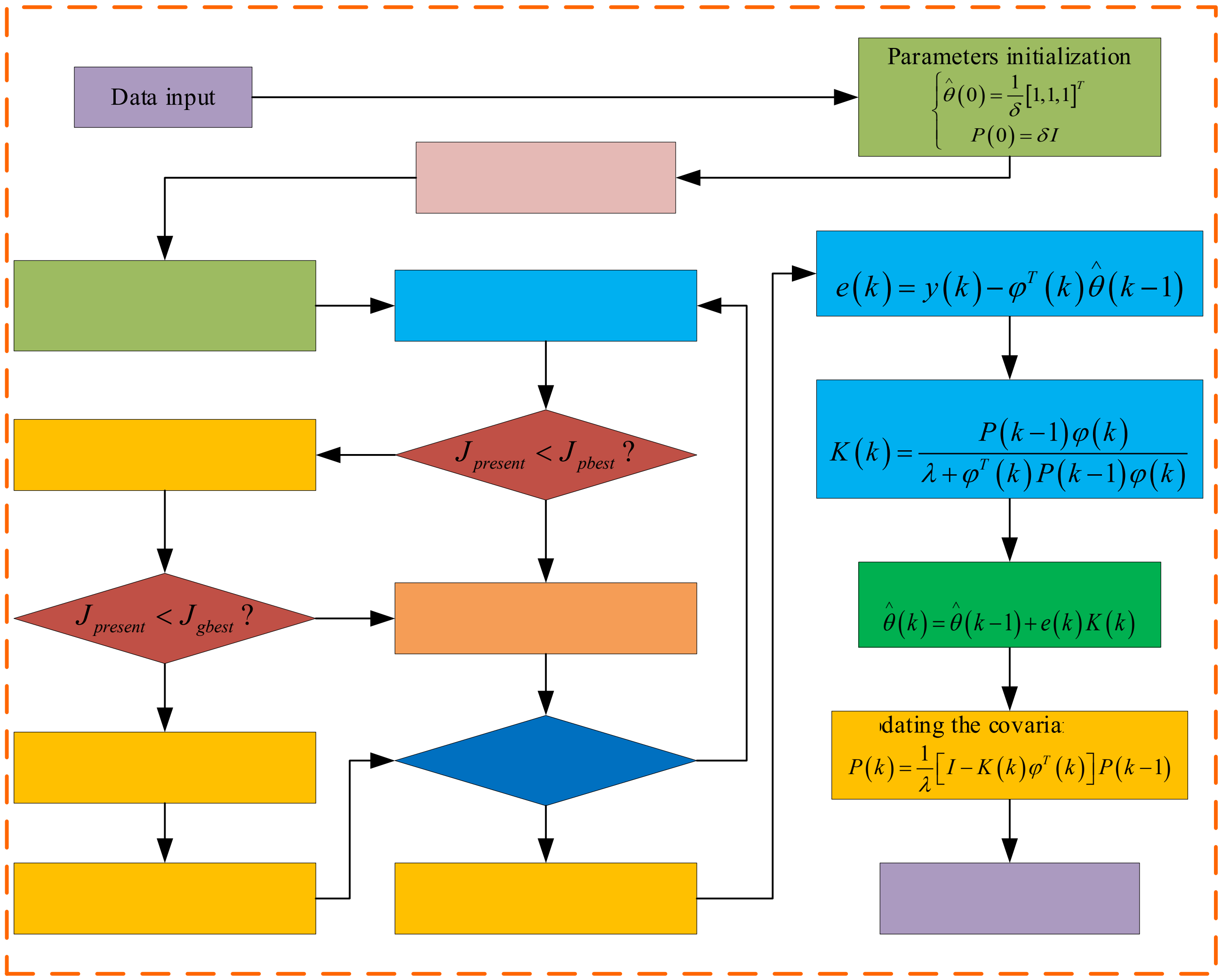

Figure 2. Parameter identification flow chart based on CFPSO-FFRLS algorithm

In Figure 2, $J_{present}$ is the present fitness value of the particle, J_{pbest} is the individual extremum, and J_{gbest} is the global extremun. The optimal value of forgetting factor is obtained by continuous optimization and iterative searching. The results of parameter identification will be utilized for subsequent SOC estimation.

2.3. AEKF algorithm with dual noise update for SOC estimation

The traditional Kalman filter is an optimal recursive data processing algorithm, which is only applicable to linear systems. For nonlinear systems such as lithium ion batteries, EKF algorithm uses Taylor formula to linearize the state space equation of the system. The state space equations of nonlinear discrete systems are generally shown in Equation (14).

$$\begin{cases} x_{k+1} = Ax_k + Bu_k + w_k \\ y_k = Cx_k + Du_k + v_k \end{cases} \tag{14}$$

In Equation (14), x_k represents the state variable at time k, y_k represents the measurement variable of the system at time k, u_k represents the input variable of the system, w_k and v_k represent the process noise and measurement noise, respectively, A is the state transition matrix, B is the input control matrix, while C and D are coefficient matrices. According to Equation (3) and (4), x_k, y_k and u_k can be defined, as shown in Equation (15), and then matrices A, B, C, and D can be obtained, as shown in Equation (16).

$$\begin{cases} x_k = \left[SOC_k, U_{1,k}, U_{2,k}\right]^T \\ u_k = I_k \\ y_k = U_k \end{cases} \tag{15}$$

$$\begin{cases} A = \begin{bmatrix} 1 & 0 & 0 \\ 0 & e^{-\frac{\Delta t}{R_1C_1}} & 0 \\ 0 & 0 & e^{-\frac{\Delta t}{R_2C_2}} \end{bmatrix} \\ B = \left[-\frac{\eta\Delta t}{Q_N},\ R_1(1-e^{-\frac{\Delta t}{R_1C_1}}),\ R_2(1-e^{-\frac{\Delta t}{R_2C_2}})\right]^T \\ C = \left[\frac{dU_{oc}}{SOC}, -1, -1\right]^T \\ D = -R_0 \end{cases} \tag{16}$$

Although the EKF algorithm optimized on the basis of Kalman filter is applicable to linear systems, it largely depends on the accuracy of the noise matrix. Therefore, in order to improve the problem of low filtering accuracy due to the inaccurate setting of the initial value of the noise covariance matrix when estimating the SOC of lithium-ion battery by the standard EKF algorithm, a dual noise update link can be introduced for noise adaption on the basis of the EKF algorithm to update the process noise and measurement noise of the EKF algorithm in real time in order to reduce the influence of noise on the estimation. The introduction of the adaptive noise link on the basis of the standard EKF algorithm can improve the algorithm's ability to adapt to noise and improve the estimation accuracy. The improved AEKF algorithm uses the noise update equations to update the process noise and measurement noise in the estimation process in real time after updating the system state variables. The SOC estimation flow chart based on the AEKF algorithm with dual noise update is shown in Figure 3.

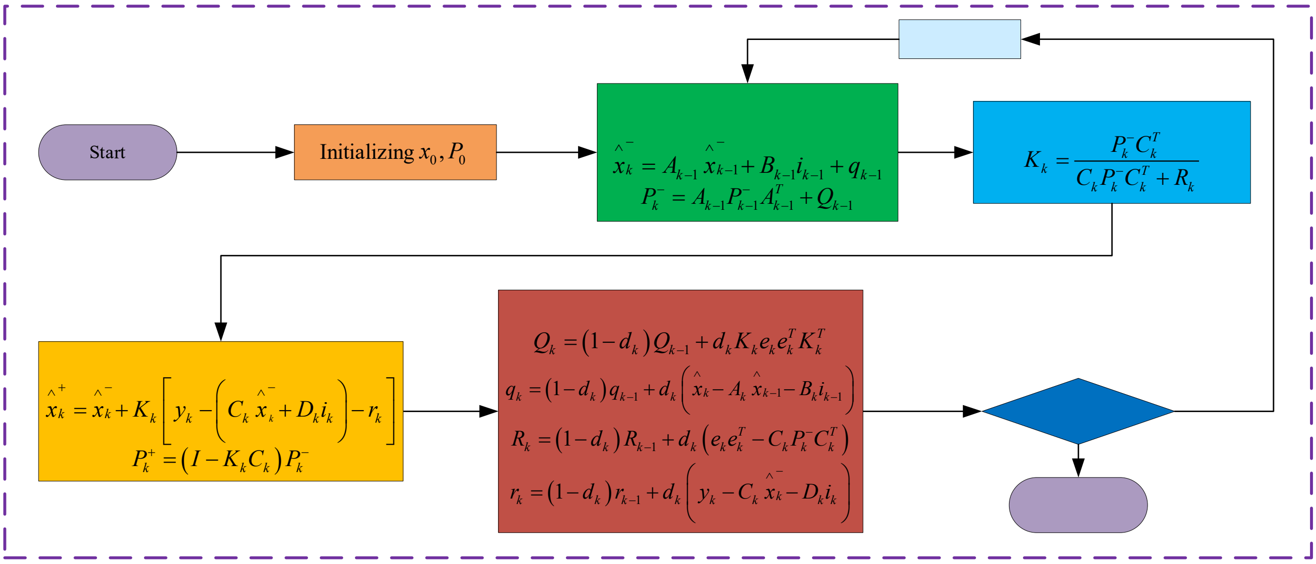

Figure 3. SOC estimation flow chart based on AEKF algorithm with dual noise update

In Figure 3, e_k is the error between simulated voltage value and actual voltage value, i is the input current value, Q represents the process noise variance, q represents the average value of process noise, R represents the measurement noise variance, r represents the average value of measurement noise, and d_k is the weighting factor of adaptive noise which is introduced to reduce the noise weight at the current moment. In the noise adaption, the weighting factor d_k is equal to $\frac{1-b}{1-b^k}$, where b is the forgetting factor for adaptive noise. In practical applications, the smaller the value of b, the smaller the impact of the previous moment. However, a smaller value of b can cause oscillations in the estimated noise, so the value should be determined according to the specific situation. By introducing the improved adaptive filtering algorithm, the statistical properties of the noise in the algorithm can be updated adaptively as the estimation results change, thus improving the estimation accuracy.

3. Analysis of experimental results

3.1. Parameter identification under different working conditions

3.1.1. Parameter identification results and analysis under HPPC working condition

In order to verify the feasibility of the improved algorithm proposed in this paper, tests need to be conducted under different working conditions. The selected ternary lithium-ion battery was first subjected to HPPC experiment at a temperature of 15°C. The optimized CFPSO-FFRLS algorithm was used to identify the parameters of second-order RC equivalent circuit model of the battery. The voltage estimation results of FFRLS, PSO-FFRLS and CFPSO-FFRLS algorithms under HPPC working condition are shown in Figure 4.

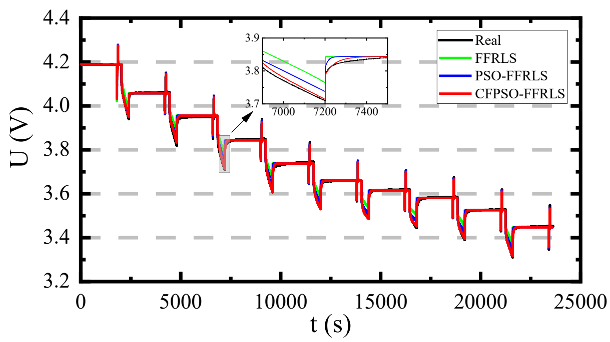

(a) Voltage estimation comparison

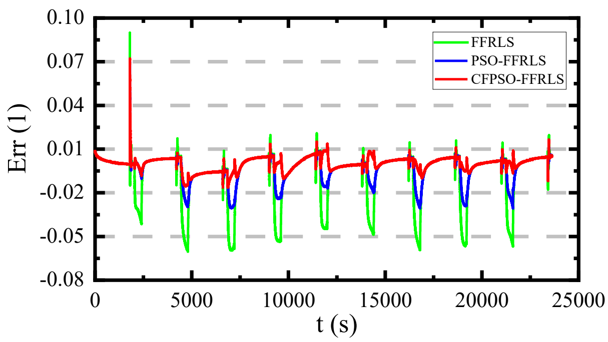

(b) Error of the voltage estimation

Figure 4. Voltage estimation results under HPPC working condition

It can be seen from Figure 4 that the proposed algorithm achieves the closest estimation result to the actual voltage value compared with the other two algorithms, with an estimation error that is effectively controlled within 2%.

In order to better compare the voltage estimation accuracy of FFRLS algorithm, PSO-FFRLS algorithm and CFPSO-FFRLS algorithm under HPPC working condition, it is necessary to compare the key data of the estimation results of the three algorithms. The three algorithms are compared through two evaluation indexes:

mean absolute error (MAE) and root mean square error (RMSE). The comparison of voltage estimation results under HPPC working condition is shown in Table 1.

Table 1. Error comparison of voltage estimation under HPPC working condition

algorithm	MAE	RMSE
FFRLS	0.98%	1.81%
PSO-FFRLS	0.58%	0.90%
CFPSO-FFRLS	0.36%	0.49%

As can be seen from Table 1, the mean absolute errors of FFRLS algorithm, PSO-FFRLS algorithm, and CFPSO-FFRLS algorithm for parameter identification under HPPC condition are 0.98%, 0.58% and 0.36%, respectively. The root mean square errors of FFRLS algorirhm, PSO-FFRLS algorithm, and CFPSO-FFRLS algorithm are 1.81%, 0.90% and 0.49%, respectively. The MAE and RMSE of the CFPSO-FFRLS algorithm are reduced by 63.27% and 72.93%, respectively. The comparison result shows that the CFPSO-FFRLS algorithm proposed in this paper has the highest estimation accuracy under HPPC working condition.

3.1.2. Parameter identification results and analysis under BBDST and DST working conditions

After getting the conclusion that the CFPSO-FFRLS algorithm has higher estimation accuracy than the other two algorithms under HPPC working condition, it is necessary to verify the validity of the algorithm under different working conditions. BBDST and DST working conditions are carried out, and the voltage estimation results under BBDST and DST working conditions are shown in Figure 5 and Figure 6.

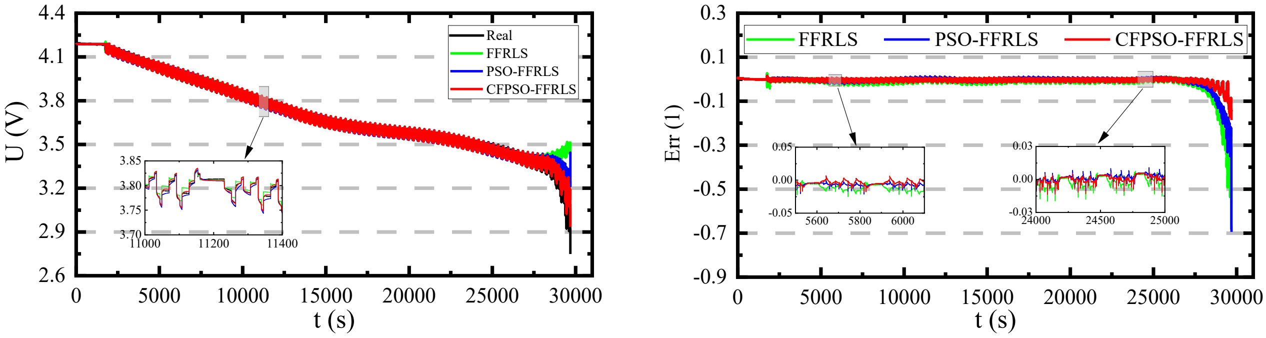

(a) Voltage estimation comparison

(b) Error of the voltage estimation

Figure 5. Voltage estimation results under BBDST working condition

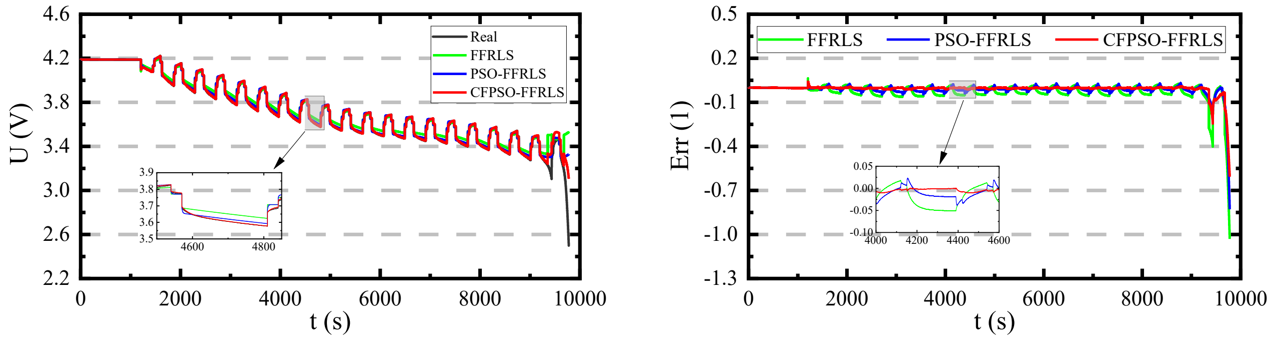

(a) Voltage estimation comparison

(b) Error of the voltage estimation

Figure 6. Voltage estimation results under DST working condition

It can be seen from Figure 5 and Figure 6 that the CFPSO-FFRLS algorithm can still accurately estimate the voltage of battery. Under both working conditions, the algorithm is still capable of maintaining the estimation error within a small range, which further verifies the accuracy of the CFPSO-FFRLS algorithm.

The comparison of voltage estimation results from two aspects under BBDST and DST working conditions is shown in Table 2.

Table 2. Error comparison of voltage estimation under BBDST and DST working conditions

algorithm	MAE		RMSE	
	BBDST	DST	BBDST	DST
FFRLS	1.65%	3.37%	5.31%	7.67%
PSO-FFRLS	0.97%	1.76%	3.24%	4.93%
CFPSO-FFRLS	0.53%	0.91%	1.43%	3.94%

It can be seen from Table 2 that the MAE and RMSE of CFPSO-FFRLS are reduced by 67.88% and 69.30% compared with the FFRLS algorithm under BBDST working condition, and the MAE and RMSE are reduced by 74.32% and 48.63%, respectively. The comparison results under BBDST and DST working conditions verify the advantages of the algorithm proposed in this paper.

3.2. SOC estimation under different working conditions

3.2.1. SOC estimation based on CFPSO-FFRLS-AEKF under HPPC working condition

After obtaining the parameter identification results under different working conditions, the parameter identification results of FFRLS are combined with EKF algorithm, while the results of PSO-FFRLS and CFPSO-FFRLS are combined with AEKF algorithm with dual noise update to estimate the SOC of lithium-ion battery, and the estimation results under HPPC working condition are obtained, as shown in Figure 7.

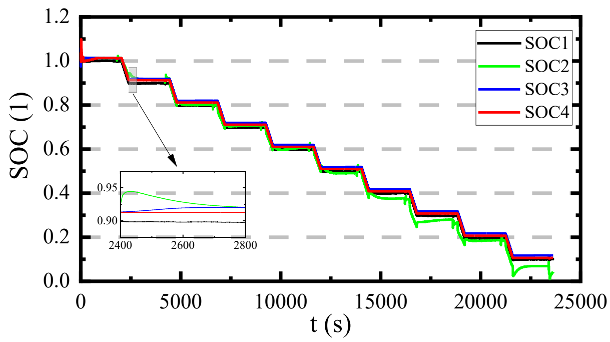

(a) Comparison of SOC estimation results

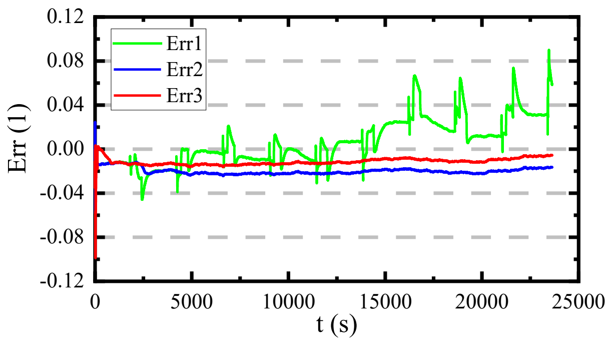

(b) Comparison of SOC estimation errors

Figure 7. SOC estimation results under HPPC working condition

In Figure 7 (a), SOC1 represents the reference value of SOC, SOC2 represents the estimated SOC value basesd on FFRLS-EKF algorithm, SOC3 represents the estimated SOC value based on PSO-FFRLS-AEKF algorithm, and SOC4 represents the estimated SOC value based on CFPSO-FFRLS-AEKF algorithm. In Figure 7 (b), Err1-Err3 represent the error of SOC estimation corresponding to SOC2-SOC4. It can be seen from Figure 7 that in the early stage of SOC estimation, since the EKF algorithm's noise covariance matrix is randomly given, its SOC estimation curve does not converge to the true SOC in time, which leads to the later estimation curve deviating more and more from the true values and gradually showing a tendency to diverge. The other two algorithms are adaptive to the noise, which makes the estimation curve converge to the true SOC value soon from the beginning and keeps a high estimation accuracy in the subsequent estimation. Because the CFPSO-FFRLS-AEKF algorithm identifies more accurate parameters, the algorithm has smaller error in estimating the SOC of lithium-ion battery.

3.2.2. SOC estimation based on CFPSO-FFRLS-AEKF under BBDST and DST working conditions

In the actual use of lithium-ion batteries, the working conditions are often more complex, and the SOC estimation is more difficult. To verify the reliability of the CFPSO-FFRLS-AEKF algorithm for estimating SOC under complex working conditions, the SOC estimation under BBDST and DST working conditions are conducted, and the estimation results are shown in Figure 8 and Figure 9.

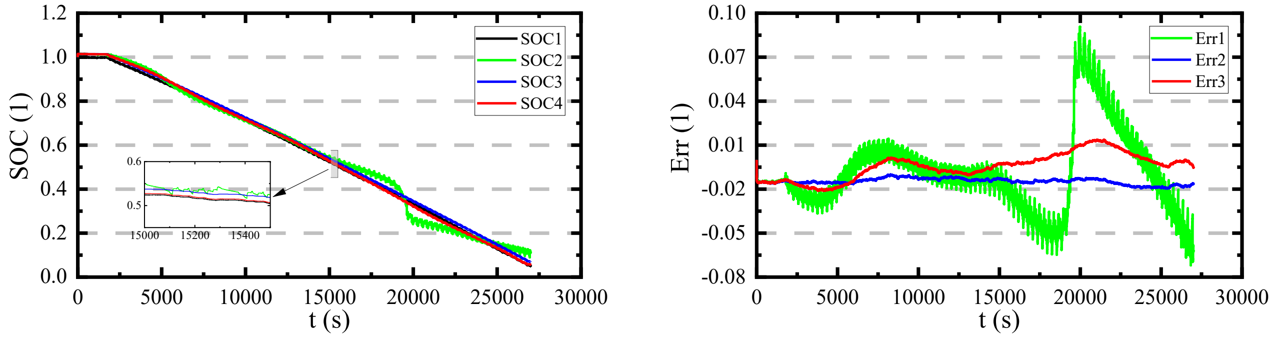

(a) Comparison of SOC estimation results (b) Comparison of SOC estimation errors

Figure 8. SOC estimation results under BBDST working condition

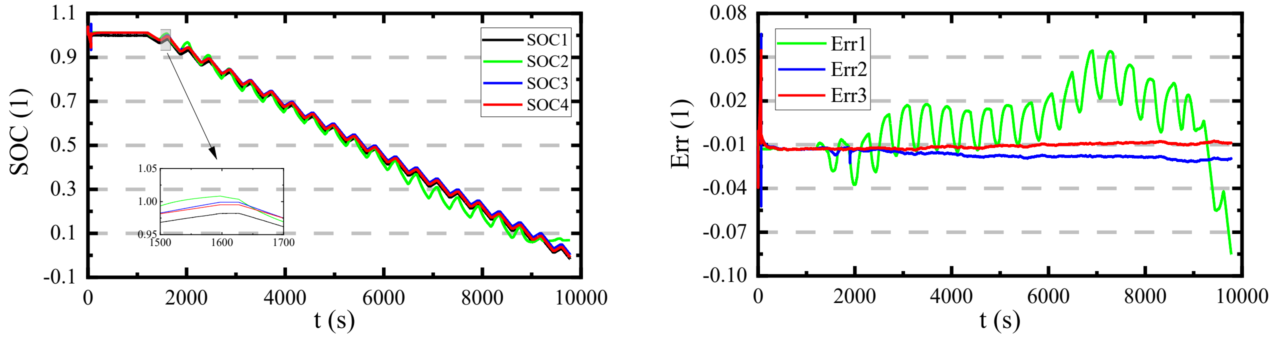

(a) Comparison of SOC estimation results (b) Comparison of SOC estimation errors

Figure 9. SOC estimation results under DST working condition

In Figure 8 (a) and Figure 9 (a), SOC1 represents the reference value of SOC, SOC2 represents the estimated SOC value basesd on FFRLS-EKF algorithm, SOC3 represents the estimated SOC value based on PSO-FFRLS-AEKF algorithm, and SOC4 represents the estimated SOC value based on CFPSO-FFRLS-AEKF algorithm. In

Figure 8 (b) and Figure 9 (b), Err1-Err3 represent the error of SOC estimation corresponding to SOC2-SOC4. As can be seen from Figure 8 and Figure 9, the error of the FFRLS-EKF algorithm gradually increases at the end of the estimation process under BBDST and DST working conditions due to the nonlinearity of the battery, while the CFPSO-FFRLS-AEKF algorithm and PSO-FFRLS-AEKF algorithm can still accurately estimate the SOC since these two algorithms possess adaptive capabilities to noise. In addition, the error curve also shows that the estimated value of CFPSO-FFRLS-AEKF algorithm quickly converges close to the true SOC value, and the algorithm maintains an estimation error of approximately 2% under BBDST working condition and around 1% under DST working condition after the algorithm converges, which is better than the other two algorithms. The results prove that the CFPSO-FFRLS-AEKF algorithm has higher estimation accuracy and better adaptability.

3.2.3. Analysis of CFPSO-FFRLS-AEKF under different working conditions

The estimated effects of the three algorithms under different working conditions are compared by two evaluation indexes, and the comparison results are shown in Figure 10.

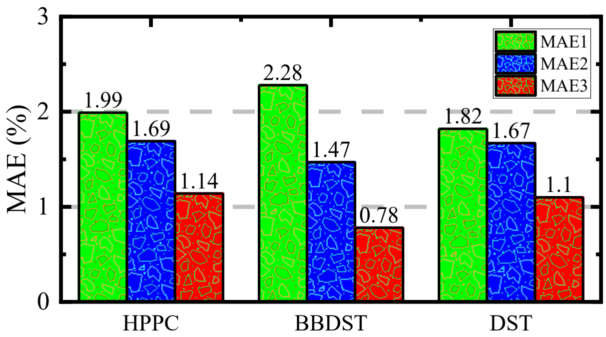

(a) Comparison of mean absolute errors under different working conditions

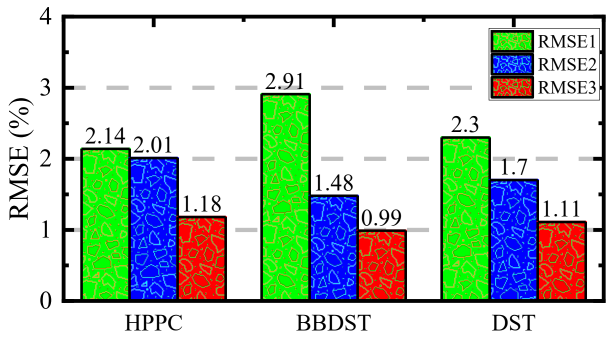

(b) Comparison of root mean square errors under different working conditions

Figure 10. Comparison of SOC estimation results of three algorithms under different working conditions

In Figure 10, MAE1 and RMSE1 represent the FFRLS-EKF algorithm, MAE2 and RMSE2 represent the PSO-FFRLS-AEKF algorithm, and MAE3 and RMSE3 represent the CFPSO-FFRLS-AEKF algorithm. It can be seen that under HPPC, BBDST and DST working condtions, the MAEs of the algorithm proposed in this paper are 1.14%, 0.78% and 1.1%, and the RMSEs are 1.18%, 0.99% and 1.11%. Under HPPC, BBDST and DST working conditions, the MAEs of CFPSO-FFRLS-AEKF algorithm are reduced by 42.71%, 65.79% and 39.56% compared with FFRLS-EKF algorithm. The RMSEs of CFPSO-FFRLS-AEKF algorithm are reduced by 44.86%, 65.98% and 51.74% under these working conditions, respectively. The results confirm the superiority of the proposed algorithm.

4. Conclusion

With the rapid development in the field of new energy, lithium-ion batteries have attracted much attention for their unique advantages and wide range of applications, and the accurate estimation of their charge state has become a major focus issue. In order to achieve high-precision SOC estimation of lithium-ion batteries, an improved CFPSO-FFRLS algorithm is proposed to identify more accurate parameters in the second-order RC model, and the joint CFPSO-FFRLS-AEKF algorithm by combining the CFPSO-FFRLS algorithm and AEKF algorithm with dual noise update is proposed for the SOC estimation. Under HPPC, BBDST and DST working conditions, the MAEs of the proposed CFPSO-FFRLS algorithm for parameter identification are 0.36%, 0.53% and 0.91%, and the RMSEs are 0.49%, 1.43% and 3.94%, respectively. The MAEs of CFPSO-FFRLS-AEKF for SOC estimation under different working conditions are 1.14%, 0.78% and 1.1%, and the RMSEs are 1.18%, 0.99% and 1.11%, respectively. The accuracy of the algorithm is greatly improved compared with the FFRLS-EKF algorithm.

In summary, the algorithm proposed in this paper provides a theoretical basis for high-precision SOC estimation of lithium-ion batteries, which is of significance for lithium-ion batteries condition monitoring. This algorithm makes an important contribution to the state estimation of lithium-ion batteries in the application of new energy vehicles.

Acknowledgements

The work was supported by the National Natural Science Foundation of China (No.62173281,61801407).

References

[1].Zhong, S. J., et al., *Recent progress in thin separators for upgraded lithium ion batteries*. Energy Storage Materials, 2021. 41: p. 805-841.

[2].Ortiz, J. P., et al., *Continual Refoircement Learning Using Real-World Data for Intelligent Prediction of SOC Consumption in Electric Vehicles*. IEEE Latin America Transactions, 2022. 20(4): p. 624-633.

[3].Wang, Z. L., et al., *A review on online state of charge and state of health estimation for lithium-ion batteries in electric vehicles*. Energy Reports, 2021. 7: p. 5141-5161.

[4].Li, J. B., et al., *Joint estimation of state of charge and state of health for lithium-ion battery based on dual adaptive extended Kalman filter*. International Journal of Energy Research, 2021. 45(9): p. 13307-13322.

[5].Cui, Z. H., et al., *A comprehensive review on the state of charge estimation for lithium-ion battery based on neural network*. International Journal of Energy Research, 2022. 46(5): p. 5423-5440.

[6].Roselyn, J. P., et al., *Optimal SoC Estimation Considering Hysteresis Effect for Effective Battery Management in Shipboard Batteries*. IEEE Journal of Emerging and Selected Topics in Power Electronics, 2021. 9(5): p. 5533-5541.

[7].Naseri, F., et al., *An Enhanced Equivalent Circuit Model With Real-Time Parameter Identification for Battery State-of-Charge Estimation*. IEEE Transactions on Industrial Electronics, 2022. 69(4): p. 3743-3751.

[8].Wang, Y. C., et al., *Research on online parameter identification and SOC estimation methods of lithium-ion battery model based on a robustness analysis*. International Journal of Energy Research, 2021. 45(15): p. 21234-21253.

[9].Chen, P. Y., et al., *Evaluation of Various Offline and Online ECM Parameter Identification Methods of Lithium-Ion Batteries in Underwater Vehicles*. ACS Omega, 2022. 7(34): p. 30504-30518.

[10].Zhang, W. J., et al., *Joint State-of-Charge and State-of-Available-Power Estimation Based on the Online Parameter Identification of Lithium-Ion Battery Model*. IEEE Transactions on Industrial Electronics, 2022. 69(4): p. 3677-3688.

[11].Xu, Y. H., et al., *Online identification of battery model parameters and joint state of charge and state of health estimation using dual particle filter algorithms*. International Journal of Energy Research, 2022. 46(14): p. 19615-19652.

[12].Xu, Y. H., et al., *State of charge estimation of supercapacitors based on multi-innovation unscented Kalman filter under a wide temperature range*. International Journal of Energy Research, 2022. 46(12): p. 16716-16735.

[13].Zhang, S. Z., & X. W. Zhang, *A comparative study of different online model parameters identification methods for lithium-ion battery*. Science China-Technological Sciences, 2021. 64(10): p. 2312-2327.

[14].Miao, H., et al., *A novel online model parameters identification method with anti-interference characteristics for lithium-ion batteries*. International Journal of Energy Research, 2021. 45(6): p. 9502-9517.

[15].Gu, T. Y., & D. Q. Wang, *A beetle antennae search optimized recurrent extreme learning machine for battery state of charge estimation*. International Journal of Energy Research, 2022. 46(13): p. 19190-19205.

[16].Sun, X. D., et al., *A novel online identification algorithm of lithium-ion battery parameters and model order based on a fractional order model*. IET Renewable Power Generation, 2021. 15(11): p. 2396-2408.

[17].Qu, D., et al., *State of charge estimation for the Vanadium Redox Flow Battery based on Extended Kalman filter using modified parameter identification*. Energy Sources Part A-Recovery Utilization and Environmental Effects, 2022. 44(4): p. 9747-9763.

[18].Shu, X., et al., *Stage of Charge Estimation of Lithium-Ion Battery Packs Based on Improved Cubature Kalman Filter With Long Short-Term Memory Model*. IEEE Transactions on Transportation Electrification, 2021. 7(3): p. 1271-1284.

[19].Tang, A. H., et al., *A multi-model real covariance-based battery state-of-charge fusion estimation method for electric vehicles using ordered weighted averaging operator*. International Journal of Energy Research, 2022. 46(12): p.

17273-17284.

[20].Xing, L. K., L. Y. Ling, & X. Y. Wu, *Lithium-ion battery state-of-charge estimation based on a dual extended Kalman filter and BPNN correction*. Connection Science, 2022. 34(1): p. 2332-2363.

[21].Shrivastava, P., et al., *Combined State of Charge and State of Energy Estimation of Lithium-Ion Battery Using Dual Forgetting Factor-Based Adaptive Extended Kalman Filter for Electric Vehicle Applications*. IEEE Transactions on Vehicular Technology, 2021. 70(2): p. 1200-1215.

[22].Lyu, X., et al., *An Adaptive and Robust UKF Approach Based on Gaussian Process Regression-Aided Variational Bayesian*. IEEE Sensors Journal, 2021. 21(7): p. 9500-9514.

[23].Gu, T. Y., et al., *The modified multi-innovation adaptive EKF algorithm for identifying battery SOC*. Ionics, 2022. 28(8): p. 3877-3891.

[24].Beelen, H., H. J. Bergveld, & M. C. F. Donkers, *Joint Estimation of Battery Parameters and State of Charge Using an Extended Kalman Filter: A Single-Parameter Tuning Approach*. IEEE Transactions on Control Systems Technology, 2021. 29(3): p. 1087-1101.

[25].Xing, L. K., et al., *State-of-charge estimation for Lithium-Ion batteries using Kalman filters based on fractional-order models*. Connection Science, 2022. 34(1): p. 162-184.

[26].Havangi, R., *Adaptive robust unscented Kalman filter with recursive least square for state of charge estimation of batteries*. Electrical Engineering, 2022. 104(2): p. 1001-1017.

[27].Pang, H., et al., *A Composite State of Charge Estimation for Electric Vehicle Lithium-Ion Batteries Using Back-Propagation Neural Network and Extended Kalman Particle Filter*. Journal of The Electrochemical Society, 2022. 169(11) : p. 1-10.

[28].Hu, C. S., et al., *State of Charge Estimation for Lithium-Ion Batteries Based on TCN-LSTM Neural Networks*. Journal of The Electrochemical Society, 2022. 169(3) : p. 1-12.

[29].Cui, X. B., & B. W. Xu, *State of Charge Estimation of Lithium-Ion Battery Using Robust Kernel Fuzzy Model and Multi-Innovation UKF Algorithm Under Noise*. IEEE Transactions on Industrial Electronics, 2022. 69(11): p. 11121-11131.

[30].Li, D., et al., *Battery Fault Diagnosis for Electric Vehicles Based on Voltage Abnormality by Combining the Long Short-Term Memory Neural Network and the Equivalent Circuit Model*. IEEE Transactions on Power Electronics, 2021. 36(2): p. 1303-1315.

[31].Deng, Z. W., et al., *Sensitivity Analysis and Joint Estimation of Parameters and States for All-Solid-State Batteries*. IEEE Transactions on Transportation Electrification, 2021. 7(3): p. 1314-1323.

[32].Peng, N., et al., *Online parameters identification and state of charge estimation for lithium-ion batteries using improved adaptive dual unscented Kalman filter*. International Journal of Energy Research, 2021. 45(1): p. 975-990.

[33].Qian, K. F., et al., *Modified dual extended Kalman filters for SOC estimation and online parameter identification of lithium-ion battery via modified gray wolf optimizer*. Proceedings of The Institution of Mechanical Engineers Part D-Journal of Automobile Engineering, 2022. 236(8): p. 1761-1774.

[34].Ouyang, T. C., et al., *Coestimation of State-of-Charge and State-of-Health for Power Batteries Based on Multithread Dynamic Optimization Method*. IEEE Transactions on Industrial Electronics, 2022. 69(2): p. 1157-1166.

[35].Ling, L. Y., & Y. Wei, *State-of-Charge and State-of-Health Estimation for Lithium-Ion Batteries Based on Dual Fractional-Order Extended Kalman Filter and Online Parameter Identification*. IEEE Access, 2021. 9: p. 47588-47602.

[36].Xu, W. H., et al., *A novel adaptive dual extended Kalman filtering algorithm for the Li-ion battery state of charge and state of health co-estimation*. International Journal of Energy Research, 2021. 45(10): p. 14592-14602.

[37].Wang, L. M., et al., *State of Charge Estimation of Lithium-Ion Based on VFFRLS-Noise Adaptive CKF Algorithm*. Industrial & Engineering Chemistry Research, 2022. 61(22): p. 7489-7503.

[38].Tian, Y., et al., *State of charge estimation of lithium-ion batteries based on cubature Kalman filters with different matrix decomposition strategies*. Energy, 2022. 238.

[39].Oh, H., J. Jeon, & S. Park, *Effects of Battery Model on the Accuracy of Battery SOC Estimation Using Extended*

Kalman Filter under Practical Vehicle Conditions Including Parasitic Current Leakage and Diffusion Of Voltage. International Journal of Automotive Technology, 2021. 22(5): p. 1337-1346.

[40].Jemmali, S., B. Manai, & M. Hamouda, *Pure hardware design and implementation on FPGA of an EKF based accelerated SoC estimator for a lithium-ion battery in electric vehicles*. IET Power Electronics, 2022. 15(11): p. 1004-1015.

[41].Sylvestrin, G. R., H. F. Scherer, & O. H. Ando, *Experimental Validation of State of Charge Estimation by Extended Kalman Filter and Modified Coulomb Counting*. IEEE Latin America Transactions, 2022. 20(11): p. 2395-2403.

[42].Ali, M. U., et al., *An adaptive state of charge estimator for lithium-ion batteries*. Energy Science & Engineering, 2022. 10(7): p. 2333-2347.

[43].Adaikkappan, M., & N. Sathiyamoorthy, *A real time state of charge estimation using Harris Hawks optimization-based filtering approach for electric vehicle power batteries*. International Journal of Energy Research, 2022. 46(7): p. 9293-9309.

[44].Huang, Z. J., Y. S. Fang, & J. J. Xu, *SOC ESTIMATION OF Li-ION BATTERY BASED ON IMPROVED EKF ALGORITHM*. International Journal of Automotive Technology, 2021. 22(2): p. 335-340.

[45].Yao, J. X., et al., *Sliding mode-based H-infinity filter for SOC estimation of lithium-ion batteries*. Ionics, 2021. 27(12): p. 5147-5157.